Contribution of cation−π interactions to the stability of Sm/LSm oligomeric assemblies

ARTICLE *in* PROTOPLASMA · NOVEMBER 2014

Impact Factor: 2.65 · DOI: 10.1007/s00709-014-0727-8 · Source: PubMed

3 AUTHORS, INCLUDING:

Milan Nikolic

University of Belgrade

21 PUBLICATIONS **116** CITATIONS

SEE PROFILE

Protoplasma
DOI 10.1007/s00709-014-0727-8

ORIGINAL ARTICLE

Contribution of cation–π interactions to the stability of Sm/LSm oligomeric assemblies

Ivana D. Mucić · Milan R. Nikolić · Srđan Đ. Stojanović

Received: 6 August 2014 / Accepted: 30 October 2014

Abstract In this work, we have analyzed the influence of cation–π interactions to the stability of Sm/LSm assemblies and their environmental preferences. The number of interactions formed by arginine is higher than lysine in the cationic group, while histidine is comparatively higher than phenylalanine and tyrosine in the π group. Arg–Tyr interactions are predominant among the various pairs analyzed. The furcation level of multiple cation–π interactions is much higher than that of single cation–π interactions in Sm/LSm interfaces. We have found hot spot residues forming cation–π interactions, and hot spot composition is similar for all aromatic residues. The Arg–Phe pair has the strongest interaction energy of −8.81 kcal mol^{-1} among all the possible pairs of amino acids. The extent of burial of the residue side-chain correlates with the ΔΔG of binding for residues in the core and also for hot spot residues cation–π bonded across the interface. Secondary structure of the cation–π residues shows that Arg and Lys preferred to be in strand. Among the π residues, His prefers to be in helix, Phe prefers to be in turn, and Tyr prefers to be in strand. Stabilization centers for these proteins showed that all the five residues found in cation–π interactions are important in locating one or more of such centers. More than 50 % of the cation–π interacting residues are highly conserved. It is likely that the cation–π interactions contribute significantly to the overall stability of Sm/LSm proteins.

Keywords Cation–π interactions · Sm/LSm proteins · Interfaces · Stabilization centers · Binding free energy

Handling Editor: Bhumi Nath Tripathi

S. Đ. Stojanović (✉)
ICTM—Department of Chemistry, University of Belgrade, Belgrade, Serbia
e-mail: srdjanst@chem.bg.ac.rs

I. D. Mucić · M. R. Nikolić
Faculty of Chemistry, University of Belgrade, Belgrade, Serbia

Introduction

Among the most important steps toward the comprehension of biological systems and processes is the understanding of noncovalent interactions (Mahadevi and Sastry 2013; Meyer et al. 2003; Waters 2004). Within these forces, an important role is played by cation–π interactions. Cation–π interactions are unique biomolecular binding forces that occur between electron-rich aromatic rings and organic or inorganic (metallic) cations. This type of noncovalent interaction can be very strong, as has been confirmed by solid-state studies of small-molecule crystal structures (Kumpf and Dougherty 1993; Zhu et al. 2004) and by theoretical and experimental analyses in the gas phase and in aqueous media (Moradi et al. 2012; Salonen et al. 2011; Zhu et al. 2004). The strength of cation–π interactions ranges between 2 and 150 kcal mol^{-1} (Priyakumar et al. 2004), which is comparable to the three other major types of molecular interactions: hydrogen bonds, van der Waals interactions, and electrostatic interactions. Cation–π interactions are therefore considered to be an essential force in generating tertiary and quaternary protein structures induced by oligomerization and protein folding (Brocchieri and Karlin 1994). While the cation–π interaction is arguably the strongest of the nonbonded interactions, its strength critically depends on the nature of aromatic system and charge of cation (Ma and Dougherty 1997). Ever since the study of cation–π interaction has gained prominence, the interplay of theory and experiments to understand the interaction in chemistry and biology has become inevitable. In a series of pioneering papers, Dougherty et al. explored the role, relevance, and range of the cation–π interaction between aromatic amino acids and side-chains of arginine and lysine (Gallivan and Dougherty 1999). Parallel to this, a series of experimental studies carried out by Amunugama and Rodgers (2003) and Huang and Rodgers (2002) explored the cation–π interaction involving alkali and alkaline metal ions and

Published online: 19 November 2014

revealed their quantitative strengths. Computations have played an important role in studying the cation–π interaction in aromatic, heteroaromatic, polycyclic aromatic compounds, and biomacromolecules (Anbarasu et al. 2009; Borozan et al. 2013; Elumalai et al. 2010; Lavanya et al. 2013; Li et al. 2009; Singh et al. 2009; Stewart et al. 2013; Vijay and Sastry 2008). While complexes with a dication have strength comparable to covalent bonds, monocationic complexes have much smaller binding energies. A strong cooperativity between cation–π, π–π, and hydrogen bonding interactions have also been observed (Reddy et al. 2008; Vijay et al. 2008). In addition to its contribution to protein stability, it has also been suggested that cation–π interaction can promote protein aggregation (Measey et al. 2009; Peter et al. 2014; Sophiya and Anbarasu 2011). These results stress the importance of cation–π interacting residues in the structural stability and specificity of proteins.

The Sm family of proteins, encompassing the Sm and Sm-like (Lsm) proteins (Seraphin 1995), are common participants in RNA metabolism in *Eubacteria* (Valentin-Hansen et al. 2004), Archaea (Fischer et al. 2010; Mura et al. 2001), and eukaryotes (Mattaj and De Robertis 1985; Zaric et al. 2005). Sm proteins primarily occur as small (~9–29 kDa) stand-alone proteins lacking other domains (Anantharaman et al. 2002) that assemble to form characteristic homomorphic or heteromorphic rings containing six or seven proteins. Members of the family are characterized by the conserved bipartite Sm domain or "Sm fold" which functions, at least in part, in binding to neighboring Sm proteins within such rings (Hermann et al. 1995; Khusial et al. 2005; Seraphin 1995). All Sm proteins form structures of a higher order which can be defined or none defined. In general, they are very stable, and sometimes, the presence of a chaotropic agent is necessary for their disruption (Zaric et al. 2005; Fischer et al. 2010). We have previously reported the contribution of hydrogen bonds, salt bridges, and noncanonical interactions to the stability of Sm oligomers (Stojanović et al. 2011; Zarić et al. 2011). In our previous work (Stojanović et al. 2010), we showed that hot spots of Sm proteins were located within densely packed regions, were highly conserved, and had large energy contributions to the interface interactions.

Many studies have analyzed the characteristics of protein–protein interfaces in an effort to search for the factors that contribute to the affinity and specificity of protein–protein interactions. This current manuscript furthers our previous work on the noncanonical interactions of Sm/LSm proteins (Stojanović et al. 2011; Zarić et al. 2011) by analyzing the same class of proteins with respect to cation–π interactions. We have systematically analyzed the influence of cation–π interactions to the stability of Sm/LSm proteins. The characteristic features of residues involved in cation–π interactions have been evaluated in terms of the distribution of cation–π interactions, interaction geometries, conservation score, energetic contribution, solvent accessibility, secondary structure, and stabilizing centers. We have focused our study at the protein interface, and hence, the cation–π interactions within a protein are not considered. The results from this study will facilitate our understanding of structure–function relationships and assist in the design and engineering of protein–protein complexes.

Materials and methods

Dataset

For this study, we used the Protein Data Bank (PDB) 08. January 2014 list of 97,746 structures (Rose et al. 2011). The selection criteria for Sm/LSm proteins to be included in the dataset were (1) no theoretical model structures and no NMR structures were accepted, these structures were not included since it was difficult to define the accuracy of the ensemble of structures in terms of displacement that was directly comparable to the X-ray diffraction studies; (2) only crystal structures with the resolution of 3.0 Å or better and a crystallographic R-factor of 25.0 % or lower were accepted; and (3) crystal structures of proteins containing Sm-like fold (SCOP classification, version 1.75) (Murzin et al. 1995) without RNA binding were accepted. Using these criteria, we created a dataset of 17 Sm/LSm proteins. The PDB IDs are as follows: 1b34, 1d3b, 1 h64, 1hk9, 1i4k, 1i8f, 1jbm, 1kq1, 1m5q, 1mgq, 1n9r, 1th7, 1u1s, 1ycy, 2vgn, 3bdu, and 3pgg.

Cation–π interaction analysis

A cation–aromatic database (CAD) (Reddy et al. 2007) was used for the calculation of various types of cation–π interactions and their geometrical features with default settings (Fig. 1). The database is searched for the instances wherein the cation is located within 6.0 Å from the centroid of the aromatic ring. This, we call it as a cation–aromatic motif, and since they all occur in a sphere of radius 6.0 Å from the centroid, we name them as the motifs present inside the sphere. A lower cutoff distance of 2.0 Å is taken to avoid the covalent bonds. The aromatic systems include the aromatic side chains of the residues tryptophan (Trp), tyrosine (Tyr), phenylalanine (Phe), and histidine (His). All the metal ions present in the database are considered as cations apart from the protonated basic amino acid residues lysine (Lys) and arginine (Arg). However, His can act either as cation or as an aromatic moiety depending on its protonation state, and in our study, both the possibilities are considered. In the case of an indole ring, the two 5- and 6-membered rings are treated individually as a π-system. This includes cation–π motifs, which are obtained by treating indole as a single entity without loss of generality. The CAD does not include asparagine (Asn) and

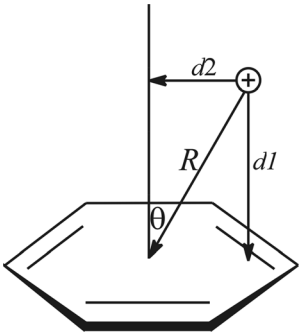

Fig. 1 Parameters for cation–π interactions: the distance (*d*1), perpendicular distance from the cation to the plane of the aromatic ring; the distance (*d*2), perpendicular distance from the cation to the principle axis of the aromatic ring; the distance (*R*) between the cation and the centroid; and the angle (θ) between the cation–centroid vector and the principle axis of the aromatic ring

glutamine (Gln) in the calculation of cation–π interactions because asparagine and glutamine can only make polar-π interactions, while arginine and lysine can participate in much stronger cation–π interactions.

Computation of cation–π interaction energy and binding free energy

We have computed the energetic contribution of all cation–π interactions for each protein in the dataset. The total interaction energy (E_{total}) has been divided into electrostatic (E_{es}) and van der Waals energy (E_{vdw}) and were computed using the program NAMD 2.8 (Phillips et al. 2005), which has implemented a subset of OPLS (Optimized Potentials for Liquid Simulations) force field to calculate the energies (Jorgensen et al. 1996). In the OPLS model, the interaction energies are represented by Coulomb and Lennard-Jones terms between sites centered on nuclei. The electrostatic energy (E_{es}) (Coulomb term) is calculated using the following equation:

$$E_{el} = q_i q_j e^2 / r_{ij} \tag{1}$$

where q_i and q_j are the charges for the atoms i and j, respectively, e is the electrostatic charge, and r_{ij} is the distance between them (measured from the center of one particle to the center of the other particle). The van der Waals energy (Lennard-Jones term) is given by

$$E_{vdw} = 4\varepsilon_{ij}\left[\left(\sigma_{ij}^{12}/r_{ij}^{12}\right) - \left(\sigma_{ij}^{6}/r_{ij}^{6}\right)\right] \tag{2}$$

where $\sigma_{ij}=(\sigma_{ii}\sigma_{ij})^{1/2}$ and $\varepsilon_{ij}=(\epsilon_{ii}\epsilon_{ij})^{1/2}$; σ and ε are the van der Waals radius (the distance at which the intermolecular potential between the two particles is zero) and dispersion well depth (a measure of how strongly the two particles attract each other), respectively (Jorgensen et al. 1996).

The change in free energy of binding (ΔΔG) was computed by the PRICE server (Guharoy et al. 2011). The contribution of a residue is computed based on the following criteria: (1) If the side chain is involved in hydrogen bonding across the interface, its contribution is based on Eq. 3 relating the ΔASA—the accessible surface area buried by the side chain (Cβ onwards)—to the ΔΔG value. (2) If there is no hydrogen bonding, but the residue belongs to the core, Eq. 4 is employed. (3) In absence of either hydrogen bonding or a location in the core, i.e., for a non-hydrogen bonded rim residue, ΔΔG=0, HBPLUS (McDonald and Thornton 1994) with its default parameters is used to identify hydrogen bonds.

$$\Delta\Delta G_{\text{calc}}\left(\text{cal mol}^{-1}\right) = 29 \times \Delta\text{ASA}_{\text{side–chain C}\beta\text{ onwards}} \tag{3}$$

$$\Delta\Delta G_{\text{calc}}\left(\text{cal mol}^{-1}\right) = 26 \times \Delta\text{ASA}_{\text{side–chain C}\beta\text{ onwards}} \tag{4}$$

Computation of conservation of amino acid residues

We computed the conservation of amino acid residues in each protein using the ConSurf server (DeLano 2002). This server computes the conservation based on the comparison of the sequence of a PDB chain with the proteins deposited in Swiss–Prot (Boeckmann et al. 2003) and finds the ones that are homologous to the PDB sequence. The numbers of PSI–BLAST iterations and the E-value cutoff used in all similarity searches were 1 and 0.001, respectively. All the sequences that were evolutionary related to each one of the proteins in the dataset were used in the subsequent multiple alignments. Based on these protein sequence alignments, the residues are classified into nine categories from highly variable to highly conserved. Residues with a score of 1 are considered to be highly variable, and residues with a score of 9 are considered to be highly conserved.

Computation of stabilization centers

Stabilization centers are the clusters of residues that make cooperative, noncovalent, and long-range interactions (Dosztanyi et al. 1997). Thus, they are likely to play an important role in maintaining the stability of protein structures. Residues can be considered as parts of stabilization centers if they are involved in medium or long-range interactions and if two supporting residues can be selected from their C- and N-terminal flanking tetrapeptides, which together with the central residues form at least seven out of the nine possible contacts. We used an online server, available at http://www.enzim.hu/scide (Dosztanyi et al. 2003), to analyze the stabilization centers of interaction-forming residues. This server defines the stabilization center based on the following criteria: (1) Two residues are in contact if there is at least one heavy atom–atom distance smaller than the sum of their van der Waals radii plus 1 Å. (2) A contact is recognized as "long-range" interaction if the interacting residues are at least ten amino acids apart. (3) Two residues form a stabilization center

if they are in long-range interaction, and if it is possible to select one–one residues from both flanking tetrapeptides of these two residues that make at least seven contacts between these two triplets (Dosztanyi et al. 2003).

Secondary structure and solvent accessibility studies

The secondary structure and solvent accessibility of amino acid residues are among the key factors that are essential for understanding the environmental and structure–function relationships of proteins. Hence, a systematic analysis of each interaction forming a residue was performed based on its location in different secondary structures of Sm/LSm proteins and their solvent accessibility. We used the program DSSP (Kabsch and Sander 1983) to obtain information about secondary structures and solvent accessibility. The secondary structures have been classified into alpha helix, beta turn, beta strand and coil, as suggested by the DSSP output. Solvent accessibility is the ratio between the solvent accessible surface area of a residue in a 3D structure and in an extended tripeptide conformation. Solvent accessibility was divided into three classes: buried (0–20 %), partially buried (20–50 %), and exposed (>50 %), indicating respectively: the least, moderate, and high accessibility of the amino acid residues to the solvent.

Results and discussion

Using the geometrical criteria described in the "Materials and methods" section, we created a dataset of 17 Sm/LSm. To reduce biased statistics caused by the lack of hetero-oligomer proteins in the dataset, we did not divide the dataset into homo and hetero sub-datasets. In order to have a nonredundant set of interfaces, we used PISCES sequence culling server (Wang and Dunbrack 2003). We excluded the interfaces that contain more than 35 % sequence identity. After the interface dataset had been assembled, several interfaces that contained ligands were rejected, leaving 215 interfaces that were actually used as the dataset in our analysis. In this study, we aimed to focus on the analysis of cation–π interactions in Sm/LSm protein interfaces. We have studied (1) distribution of cation–π interactions, (2) interaction geometries, (3) energetic contribution of cation–π interactions, (4) solvent accessibility of amino acids and binding free energy, and (5) secondary structure preferences and stabilization center residues.

Distribution of cation–π interactions

The distribution of cation–π interactions is shown in Table 1, based on data in Sm/LSm protein interfaces in our dataset. There were a total of 181 interactions. Some of the interfaces have no interactions, while most of them have a dozen interactions (the structures with PBD ID codes 1h64, 1i4k, 1jbm, 1m5q, and 1th7).

Table 1 Frequency of occurrence of cation–π interaction forming residues at Sm/LSm protein interfaces

	N^a	$\%^b$	$N_{cat-\pi}{}^c$	$\%_{cat-\pi}{}^d$	$N_{hot\ spot}{}^e$	$\%_{hot\ spot}{}^f$
Amino acid						
Arg	754	8.1	84	23.5	22	12.6
Lys	604	6.5	18	5.1	7	4.1
His	310	3.3	124	34.7	45	25.9
Phe	445	4.8	57	16.0	54	31.0
Tyr	386	4.1	74	20.7	46	26.4
Total	2499	26.8	357	100	174	100
Pair (cation–π)						
Arg–His	–	–	2	1.1	1	0.9
Arg–Phe	–	–	39	21.5	39	36.4
Arg–Tyr	–	–	43	23.8	18	16.8
Lys–His	–	–	14	7.7	7	6.5
Lys–Phe	–	–	1	0.6	1	0.9
Lys–Tyr	–	–	3	1.7	0	0
His–His	–	–	29	16.0	0	0
His–Phe	–	–	17	9.4	14	13.2
His–Tyr	–	–	28	15.4	27	25.3
Cd^{2+}–His	–	–	5	2.8	–	–
Total	–	–	181	100	107	100

[a] The number of amino acid in whole database

[b] Percent of amino acid in whole database

[c] Number of cation–π interactions in Sm/LSm protein interfaces

[d] Percent of cation–π interactions in Sm/LSm protein interfaces

[e] The number of hot spot amino acid in cation–π interaction forming residues

[f] Percent of hot spot amino acid in cation–π interaction forming residues

We have computed the composition of cation–π interaction forming amino acids using protein sequences in the 215 Sm/LSm protein interfaces. The number and composition of each amino acid are presented in Table 1. We observed that Phe had the highest occurrence among the aromatic residues involving in cation–π interactions. Arg was higher than Lys among the cationic residues in the set of Sm/LSm proteins studied. This result is consistent with earlier report on Sm/LSm proteins (Stojanović et al. 2010). The number of cation–π interactions exhibited by each of the amino acid is included in Table 1. The contribution of Arg was five times that of Lys. It might be due to the fact that the side-chain of arginine is larger and less well water-solvated than that of other amino acid residues, it likely benefits from better van der Waals interactions with the aromatic ring. In the work presented by Crowley and Golovin (2005), it was found that cation–π interactions involving Arg were common in the interfaces of protein complexes. Among the aromatic residues, His was the most common amino acid involved in such

interactions. His can act either as cation or as an aromatic moiety depending on its protonation state, and in our study, both the possibilities are considered.

There are ten cation–π interacting pairs depicted in Table 1. It was found that among the cation–π interactions involving Arg residues, Arg–Tyr residues showed the highest percentage of interaction compared with Arg–Phe and Arg–His interactions. Among the cation–π interactions involving Lys residues, Lys–His interaction was higher than Lys–Phe and Lys–Tyr interactions. Considering His, pair His–His had the highest contribution followed by His–Tyr. It is interesting to note that even though, individually, Arg and Phe exhibited higher cation–π interactions, but as pairs, Arg–Tyr were involved in more number of cation–π interactions than the other nine pairs. Hence, the Arg–Tyr, Arg–Phe, His–His, and His–Tyr interactions may be quite important in the stability of these Sm/LSm proteins. These results are comparable with the results observed in β-lactamases (Lavanya et al. 2013), RNA-binding proteins (Anbarasu et al. 2007), immunoglobulin proteins (Tayubi and Sethumadhavan 2010), sugar-binding proteins (Elumalai et al. 2010), and metalloproteins (Anitha et al. 2012).

We have found five (2.8 %) cation–π interactions between Cd^{2+} metal cations and the π systems of surrounding amino acids. The interactions involve His amino acid residues as the π systems. The unique structure of histidine makes it play multiple roles in the molecular interactions. The coordinate interactions between histidine and metallic cations are the strongest ones acting in broad range, followed by the cation–π, hydrogen–π, and π–π stacking interactions (Liao et al. 2013). Cation–π interactions between metal cations and π systems recently emerged as one of the fundamental bonding motifs of key importance in molecular recognition (Chaturvedi and Shrivastava 2005; Salgado et al. 2007; Zhang et al. 2007).

We analyzed the interface hot spot residues in subunits of Sm/LSm proteins in an attempt to understand the high stability of Sm/LSm protein associations. Studies of protein interfaces have revealed that binding energies are not uniformly distributed. Instead, there are certain critical residues called hot spots that comprise only a small fraction of the interface but account for the majority of the binding energy (Bogan and Thorn 1998; Moreira et al. 2007). We found 174 (48.8 %) hot spot residues forming cation–π interactions and that the hot spot composition is similar for all aromatic residues (Table 1). On the other hand, the cationic residues Lys and Arg had smaller occurrence in hot spots. A possible explanation for this is that amino acids that are capable of undergoing multiple types of favorable interactions are preferred as hot spots.

In our analysis, we investigated multiple cation–π interactions, an illustrative example is shown in Fig. 2. Cation groups from Arg34 and Arg64 can interact with the aromatic ring of Tyr78 simultaneously. This type of interaction is marked as

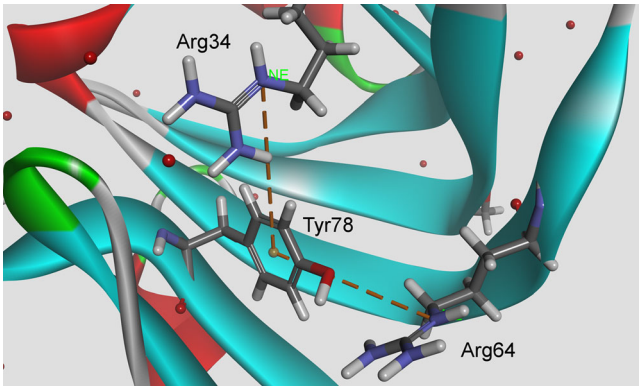

Fig. 2 Details of multiple cation–π interactions of Putative snRNP Sm-like protein from *Methanobacterium thermautotrophicum* (PDB ID code 1jbm). The cation–π interactions are marked with *brown dashed lines* (C:Arg34:NE–B:Tyr78; C:Arg64:NE–B:Tyr78). Figure was prepared using the program Discovery Studio Visualizer 4.0 (Accelrys Software Inc. 2013)

furcation. The analysis shows that about 30 % of the total interactions in the dataset are involved in the formation of multiple cation–π interactions. This means that furcation is an inherent characteristic of macromolecular crystal structures (Stojanović et al. 2012). The furcation level of multiple cation–π interactions is much higher than that of single cation–π interactions in Sm/LSm protein interfaces. The majority of furcated interactions exhibit longer distances than the simple non-furcated interactions as expected (Dimitrijević et al. 2012).

We used the ConSurf server to compute the conservation score of residues involved in cation–π interactions in Sm/LSm protein interfaces. Among the cationic residues, 52.5 % of them had a conservation score of ≥6, the cutoff value used to identify the stabilizing residues. Twelve of the residues had the highest score of 9. Additionally, most of the additional residues comprising the interfaces also show a great degree of conservation. Analysis of the conservation patterns of cation–π interactions showed that multiple interactions (54.8 %) are conserved more than single interactions (45.2 %), and it is considered that structurally conserved residues are important in protein stability and folding (DeLano 2002). This trend is similar to those observed in β-lactamases (Lavanya et al. 2013), immunoglobulin proteins (Tayubi and Sethumadhavan 2010), sugar-binding proteins (Elumalai et al. 2010), metalloproteins (Anitha et al. 2012), and therapeutic proteins (Shanthi et al. 2009). Hence, the level of evolutionary conservation was used often as an indicator for the importance of the position in maintaining the protein's structure and/or function.

Interaction geometries

The geometrical details of residues forming cation–π interactions are quantified in terms of the parameters (R, θ) described

in the methodology. The frequency distribution of the distance and angle parameters of cation–π interaction pairs is analyzed (Fig. 3).

The plot of distance distribution (R) derived from cation–π interaction pairs (Fig. 3a) shows the prominent peak centered at 5 Å. There is no significant statistical difference in the distribution of R between the multiple and the single cation–π interactions. Some of interactions are quite long (>5.5 Å), but they are well behaved; in this respect, they may be termed weak rather than bad. The fluctuations are clearly a consequence of their greater flexibility. The analysis of the geometry of the cation–π interactions has revealed that the angle (θ) value falls into distinct ranges corresponding to the multiple (70–90°) and single (20–50°) cation–π interactions (Fig. 3b). There is a significant statistical difference in the angle distribution between the multiple and the single cation–π interactions. In general, the separation distance between the cation group and the aromatic ring decreases as the angle decreases. The geometries that are observed in abundance are not necessarily the ones that have the highest interaction energy between the two moieties in a pair, but the ones that can provide the maximum overall stability to the protein structure by the optimum use of all cation–π interactions. These results were consistent with the results observed with protein–porphyrin complexes (Dimitrijević et al. 2012).

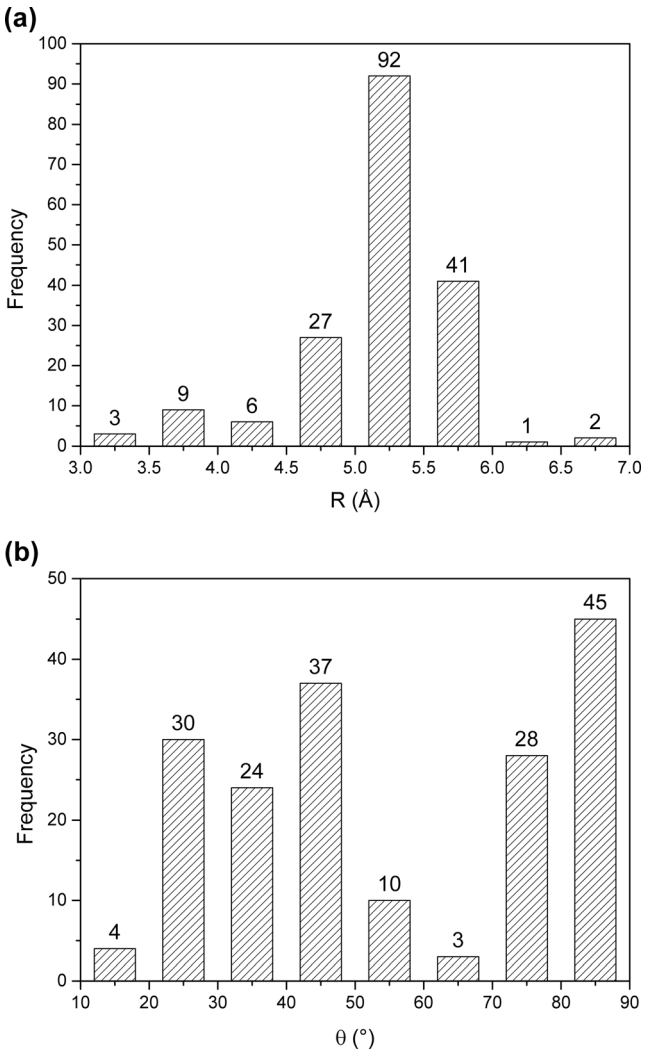

Fig. 3 Interaction geometries. **a** Distance distribution of cation–π interactions. **b** θ angle distribution of cation–π interactions

Energetic contribution of cation–π interactions

To estimate the stabilization energy of the different cation–π pairs identified in X-ray Sm/LSm interfaces, energy calculations were performed. In our database, it was found that cation–π interactions had less than −20 kcal mol^{-1} energy, and most of them had energy in the range from −3 to −8 kcal mol^{-1}. It has been reported that in globular proteins, roughly one quarter and in membrane proteins 65 % of the cation–π interactions have an energy less than −4 kcal mol^{-1} (Gallivan and Dougherty 1999; Gasymov et al. 2012; Gromiha 2003; Lavanya et al. 2013; Ramanathan et al. 2011).

We have calculated the average interaction energy for all possible interaction pairs, and the results are presented in Table 2.

It is noteworthy that the interaction energy is mainly due to the electrostatic term (E_{es}), and the contribution from van der Waals energy term (E_{vdw}) is very minimal. Electrostatic attraction between the π system and the cation has been established as the main contributing force to the interaction (Ma and Dougherty 1997; Salonen et al. 2011). The energy of cation–π interaction depends upon various factors such as the size and electronic structure of the cation, nature of the π-ligand, and extent of ligation (Hallowita 2011; Mahadevi and Sastry 2013). In terms of energetically significant interactions with π residues in the study group, the energies from Arg interactions are higher when compared with Lys and His interactions with π residues. This phenomenon may be due to the fact that the side-chain of Arg is larger and less well water-solvated than that of Lys, it likely benefits from better van der Waals interactions with the aromatic ring (Gallivan and Dougherty 1999). In addition, the side-chain of Arg may still donate several hydrogen bonds while simultaneously binding to an aromatic ring, whereas Lys would typically have to relinquish hydrogen bonds to bind to an aromatic (Mitchell et al. 1994). On an average, Arg–Phe has the strongest cation–π interaction energy of –8.81 kcal mol^{-1}. These results clearly indicate that cation–π interactions involving Arg provide stabilizing contributions to the Sm/LSm protein association. The cation–π interaction energy of protonated histidine (His^+) is smaller than other two cationic residues (Arg and Lys) because in protein structures, the histidine frequently and reversibly transforms from neutral form to protonated form

Table 2 Cation–π interaction energetic contribution for the interacting residue pairs

Interacting pair	N[a]	E_{es}[b] (kcal mol^{-1})	E_{vdw}[c] (kcal mol^{-1})	E_{total}[d] (kcal mol^{-1})
Arg–His	2	−7.06 (1.4)	−0.15 (0.1)	−7.21 (1.5)
Arg–Phe	39	−8.86 (1.5)	0.05 (0.4)	−8.81 (1.4)
Arg–Tyr	43	−2.91 (1.1)	−0.12 (0.1)	−3.03 (1.1)
Lys–His	14	−5.04 (1.3)	−0.40 (0.5)	−5.44 (1.3)
Lys–Phe	1	−5.55	−0.09	−5.64
Lys–Tyr	3	−1.31 (0.2)	−0.03 (0.0)	−1.34 (0.2)
His–His	29	−4.52 (0.5)	−0.23 (0.0)	−4.75 (0.5)
His–Phe	17	−5.62 (0.8)	−0.26 (0.1)	−5.88 (0.8)
His–Tyr	28	−0.91 (0.1)	−0.21 (0.0)	−1.12 (0.1)
Cd^{2+}–His	5	−22.07 (0.9)	−0.01 (0.0)	−22.08 (0.9)

[a] Number of interactions
[b] Electrostatic energy
[c] van der Waals energy
[d] Total interaction energy
The standard deviations are given in parenthesis

(Liao et al. 2013). We found that there are no favorable cation–π interactions between the Tyr and other residues. Statistically, Tyr cation–π pairs are less energetically significant compared to others. Indeed, the binding energies of Lys–Tyr and His–Tyr pairs are an average value close to −1 kcal mol^{-1}. These results were consistent with the results observed with protein–porphyrin complexes (Dimitrijević et al. 2012), protein–DNA complexes (Gromiha et al. 2004), prokaryotic and eukaryotic translation elongation factors (Anbarasu et al. 2009), lipocalins (Gasymov et al. 2012), and β-lactamase (Lavanya et al. 2013).

Generally speaking, in gas phase, cation–π interaction energies of metallic cations are larger than those of organic cations (protonated amino acids); however, in the aqueous solution, the cation–π interaction energies of organic cations are larger than those of metallic cations (Mahadevi and Sastry 2013). The cation–π energy (−22 kcal mol^{-1}) of Cd^{2+} is much larger than those of other cations because the 4D valence orbitals of Cd^{2+} can make stronger bonding molecular orbitals (MO) with the π-MO of aromatic residues. These results show the vital role played by metallic cations for the contribution to cation–π interactions.

Solvent accessibility of amino acids and binding free energy

An interesting question concerns the location of cation–π interactions within protein structures. Cationic residues generally prefer to be on the surface of proteins whereas aromatic amino acids prefer to remain in the hydrophobic core. Because a cation–π interaction contains both a cation and an aromatic, it is not clear whether the interacting pairs should prefer to be located on the surfaces of proteins or in the cores. Traditional methods for determining residue surface accessibility rely on calculating the water-exposed surface area for a given amino acid. Because cation–π partners are necessarily in contact with one another, their water-accessible surface is diminished, even though the interacting pair as a unit may be well solvated. We observed that Arg and Lys preferred to be in an exposed region, whereas His preferred to be in a partially buried region, while Phe and Tyr preferred to be in a buried region. This observation is quite reasonable in the sense that the aromatic residues are in principle, nonpolar residues, and tend to be buried. Since Arg and Lys are polar in nature, they tend be exposed to the solvent surface. The polar residues might contribute significantly to the stability of the Sm/LSm proteins as the contribution of the global energy is much greater in solvation. However, these observations were consistent with the results observed with cation–π pairs in β-lactamases (Lavanya et al. 2013), immunoglobulin proteins (Tayubi and Sethumadhavan 2010), sugar-binding proteins (Elumalai et al. 2010), metalloproteins (Anitha et al. 2012), and therapeutic proteins (Shanthi et al. 2009).

Residues making critical interactions in the interface are usually well conserved in evolution and also contribute significantly to the binding free energy. Residues in the core of interface are usually more conserved than those in the rim, and the contribution of core residues to the change in free energy of binding (ΔΔG) correlates well with and can be quantified as a function of the loss of accessible surface area (ΔASA), due to side-chain burial. The ΔΔG is an indicator of the energetic importance of a given interface residue to the binding process (Guharoy and Chakrabarti 2009). Hence, we have used the quantitative relationships between ΔΔG and ΔASA of interface cation–π interaction-forming residues to estimate the contribution of a residue to the free energy of binding (Fig. 4).

We observe a strong correlation (R=0.985) between ΔASA and ΔΔG for the interface core, but not the rim (0.850), and it yielded a slope of 24 cal mol^{-1} Å^2 (Fig 4a). We had also found a strong correlation (R=0.997) between ΔASA and ΔΔG for hot spot residues as opposed to non-hot spot ones. Figure 4b yields a value of the energetic contribution to be 25 cal mol^{-1} per Å^2. The change in side-chain solvent accessible area (ΔASA) of interface residues has been related to change in binding energy due to mutating interface residues to Ala (ΔΔG). The extent of burial of the residue side-chain correlates with the ΔΔG of binding for residues in the core and also

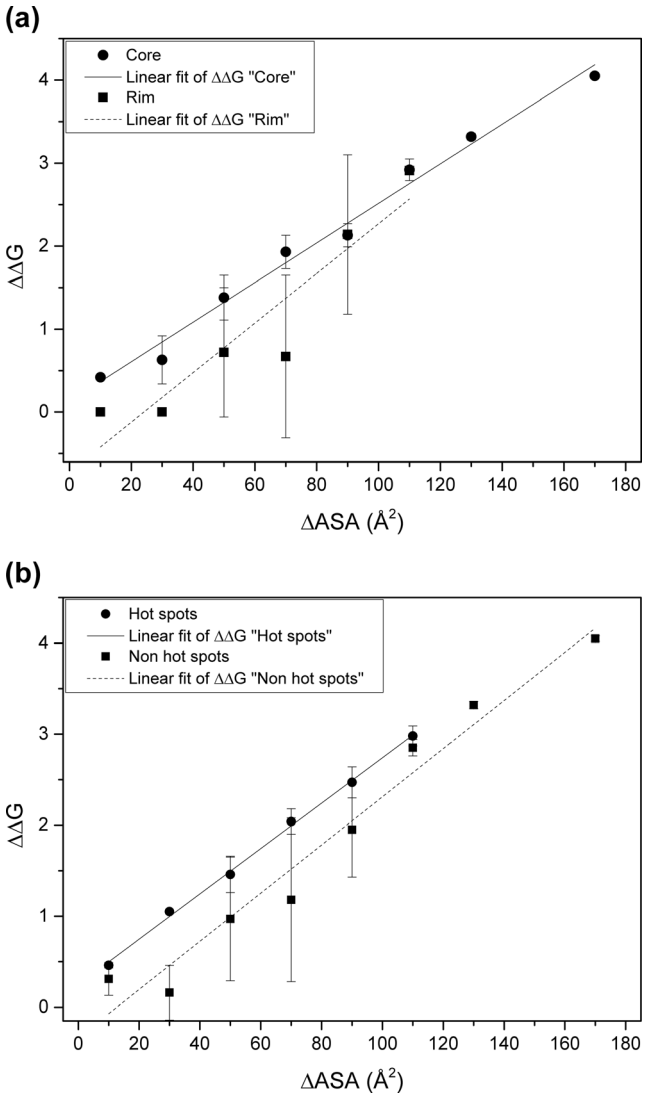

Fig. 4 Relationship between ΔASA and the change in free energy of binding (ΔΔG) of cation–π interaction forming residues. Along the x-axis, all of the values in a bin (size 20 Å^2) are pulled together and shown in the middle, while the y value corresponds to the mean of their ΔΔG values (the *vertical bars* representing the standard deviations). **a** Values for the core and rim residues. **b** Values for the hot spot and non-hot spot residues

for hot spot residues cation–π bonded across the interface. In general, hot spots contribute larger ΔASA relative to non-hot spot residues. The residues that are important for binding energetics tend to occur more near the center (core) of the interface than at its edges (rim). These results are comparable with the results observed in structures of protein–protein complexes (Guharoy and Chakrabarti 2009).

Secondary structure preferences and stabilization center residues

The propensity of the amino acid residues to favor a particular conformation is well described. Such a conformational preference is dependent not only on the amino acid alone but also on the local amino acid sequence (Chakkaravarthi et al. 2006). In order to obtain the preference and pattern of each cation–π interaction-forming residue in Sm/LSm interfaces, we conducted a systematic analysis based on their location in different secondary structures. We have calculated the occurrence of cation–π interaction-forming residues in different secondary structures in our data set which classify amino acids into helix, strand, and turn, and the results are presented in Table 3.

It was found that cationic residues such as Arg and Lys preferred to be in strand. In the aromatic group, it was found that His preferred to be in helix, Phe preferred to be in turn, and Tyr preferred to be in strand. It is interesting to note that these results were not consistent with the results observed with cation–π pairs in β-lactamases (Lavanya et al. 2013), immunoglobulin proteins (Tayubi and Sethumadhavan 2010), sugar-binding proteins (Elumalai et al. 2010), metalloproteins (Anitha et al. 2012), and therapeutic proteins (Shanthi et al. 2009). Most of the anion–π interactions between the residues prefer the secondary structure of strand segments, which is not surprising because strands represent the majority of secondary structures of Sm/LSm proteins. Hence, the preference of an amino acid to form cation–π interaction in a particular secondary structure is not the same as the preference of the amino acid for a particular secondary structure (Malkov et al. 2008). This analysis indicates that the cation–π interactions do not occur at random but have a residue-specific preference for a particular secondary structure.

Stabilization centers (SC) are composed of certain clusters of residues, involved in the cooperative long-range interaction of proteins that regulate flexibility, rigidity, and stability of protein structures. Stabilization centers are important in regulating the turnover of certain proteins by preventing their decay with cooperative long-range interactions. The most frequent stabilization center residues are usually found at buried positions and have a hydrophobic or aromatic side-chain, but some polar or charged residues also play an important role in stabilization. The stabilization centers show a significant difference in the composition and in the type of linked secondary structural elements, when compared with the rest of the residues.

Table 3 Frequency of occurrence of cation–π interaction forming residues in different secondary structures

Amino acid	Helix (%)	Strand (%)	Turn (%)
Arg	13.3	66.7	20.0
Lys	40.3	58.1	1.6
His	57.7	37.4	4.9
Phe	0.0	33.9	66.1
Tyr	34.3	62.9	2.8

The performed structural and sequential conservation analysis showed a higher conservation of stabilization centers over protein families (Dosztanyi et al. 1997; Magyar et al. 2005). In addition, sequence and structure motifs have an application in drug design (Craik et al. 2001).

We have computed the stabilization centers for all cation–π interaction-forming residues in Sm/LSm interfaces. Table 4 shows the percentage contribution of the individual amino acid residue which is part of the stabilizing center involved in cation–π interactions.

Considering the whole data set, 111 (31.1 %) stabilizing residues are involved in building cation–π interactions. It was found that 21.6 % of cationic residues and 34.9 % of π residues were found to have one or more stabilization centers which is in accordance with the percentage share of stabilization centers in β-lactamases (Lavanya et al. 2013) and RNA-binding proteins (Anbarasu et al. 2007). π residues were found to have more stabilization centers than cationic residues. Lys was found to have somewhat more stabilization centers than Arg residues in Sm/LSm interfaces. Among the stabilization centers involving π residues, Tyr showed the highest contribution (93.2 %). This could be explained by the fact that Tyr residues preferred to be in buried region (Materials and methods). It was interesting to note that all the five residues found in cation–π interactions are important in locating one or more stabilization centers. These observations strongly reveal that these residues may contribute significantly to the structural stability of these proteins in addition to participating in cation–π interactions.

An illustrative example of cation–π interaction involving more stabilization centers is shown in Fig. 5. A cation group from Arg4 interacts with π-system of Tyr34. The three stabilization centers are indicated by wire-meshed surface (red labels). The residue Arg4 is part of K34 stabilization center while Tyr34 is part of J4 and K9 stabilization centers.

Table 4 Involvement of stabilizing center residues in cation–π interactions of Sm/LSm interfaces

Amino acid	$N_{cat-\pi}$ [a]	SC [b]	$SC_{\%}$ [c]
Cationic			
Arg	84	15	17.9
Lys	18	7	38.9
Total	102	22	21.6
π residues			
His	124	5	4.0
Phe	57	15	26.3
Tyr	74	69	93.2
Total	255	89	34.9

[a] Number of cation–π interactions in Sm/LSm protein interfaces

[b] Number of SC residues involved in cation–π interactions

[c] % of SC residues involved in cation–π interactions

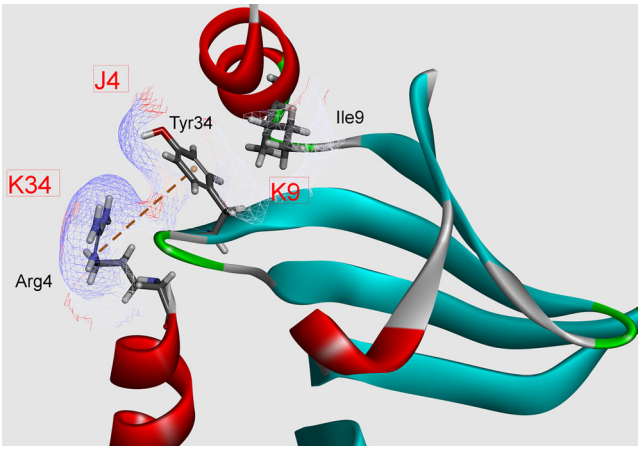

Fig. 5 Details of cation–π interaction involving more stabilization centers at the interface of Putative snRNP Sm-like protein from *Pyrococcus abyssii* (PDB ID code 1h64). The cation–π interaction is marked with a *brown dashed line* (J:Arg4:NE–K:Tyr34). Figure was prepared using the program Discovery Studio Visualizer 4.0 (Accelrys Software Inc. 2013)

All above studies showed that there exist different types of cation–π interactions, which disclosed the structure properties, binding strength, and components of cation–π interactions. The research results on cation–π interactions make an important contribution in finding new ligand binding sites, designing new ligands and drug molecules, as well as designing functional peptides and engineering modified proteins. In the past decade, mounting experimental evidence for cation–π interaction has been forthcoming. In gas phase, the early pioneering experimental studies of cation–π interaction were carried out by HPMS (high-pressure mass spectrometry), Fourier transform ion cyclotron resonance (FT-ICR) as well as IR (infrared spectroscopy) techniques. The experimental studies in solution and solid phases for cation–π interactions were mainly through NMR (nuclear magnetic resonance), UV (ultraviolet spectroscopy), CD (circular dichroism), electrospray ionization Fourier transform mass spectrometry (ESI-MS) studies, microcalorimetry as well as X-ray methods (Mahadevi and Sastry 2013). Thus, different spectroscopy techniques have emerged as reliable sources of information on the cation–π interaction. Investigation of cation–π interactions also aids in a further understanding of why nature selects aromatic amino acids as fundamental building blocks of life.

Conclusions

We have systematically analyzed the influence of cation–π interactions to the stability of Sm/LSm assemblies. Further, the characteristic features of residues involved in cation–π interactions have been evaluated in terms of the distribution of cation–π interactions, conservation score, interaction geometries, energetic contribution, solvent accessibility, binding

free energy, secondary structure preferences, and stabilization center residues.

We have found that most of the Sm/LSm interface residues exhibit cation–π interactions. The side chain of Arg is more likely to be in cation–π interactions than Lys in the cationic residues. His has the highest occurrence in these interactions compared with the other two π residues, Phe and Tyr. Among the cation–π residue pairs that were involved in these interactions, the Arg–Tyr residue pair showed the maximum number of cation–π interactions and the Lys–Phe pair showed the minimum number of interactions. The furcation level of multiple cation–π interactions is much higher than that of single cation–π interactions in Sm/LSm interfaces. Analysis of conservation patterns of cation–π interactions has shown that the multiple interactions have been conserved more than the single interactions. We have found hot spot residues forming cation–π interactions and that the hot spot composition is similar for all aromatic residues. On the other hand, the cationic residues Lys and Arg occur less in hot spots. Analysis of cation–π interaction energy revealed that there is stronger electrostatic energy than van der Waals energy and the influence of Arg is higher than Lys, indicating the difference in geometric features of Arg and Lys side chains. The cation–π interaction energy shows that Arg–Phe energy is the strongest, and His–Tyr is the lowest among the ten possible pairs in the 215 Sm/LSm interfaces investigated. It is found that in the Sm/LSm interfaces, the positively charged amino acids, Arg and Lys, involved in cation–π interactions, prefer to be in the solvent-exposed surface, whereas His preferred to be in the partially buried region, while Phe and Tyr preferred to be in the buried region. The change in side-chain solvent accessible area (ΔASA) of interface residues has been related to change in binding energy due to mutating interface residues to Ala (ΔΔG). In the secondary structure arrangement of cationic group, Arg and Lys preferred to be in strand. In the aromatic group, it was found that the His prefers to be in helix, Phe prefers to be in turn, and Tyr prefers to be in strand. We have found that significant numbers of residues have one or more stabilization centers and thus provide additional stability to the Sm/LSm proteins.

In conclusion, the results obtained in this study have identified cation–π interactions that contribute to the stabilization of the Sm/LSm assemblies. They will facilitate our understanding of structure–function relationships and assist in the design and engineering of protein–protein complexes.

Acknowledgments This work was supported by the Ministry of Education, Science and Technological Development of the Republic of Serbia (Grants Nos. 172001, 172035). The authors are grateful to Dr. David R. Jones for proofreading the manuscript.

Conflict of interest The authors declare that they have no conflict of interest.

References

Accelrys Software Inc (2013) Discovery studio visualizer, release 4.0. Accelrys Software Inc, San Diego

Amunugama R, Rodgers MT (2003) Influence of substituents on cation–π interactions: 5. Absolute binding energies of alkali metal cation–anisole complexes determined by threshold collision-induced dissociation and theoretical studies. Int J Mass Spectrom 222:431–450

Anantharaman V, Koonin EV, Aravind L (2002) Comparative genomics and evolution of proteins involved in RNA metabolism. Nucleic Acids Res 30:1427–1464

Anbarasu A, Anand S, Mathew L, Sethumadhavan R (2007) Influence of cation–π interactions on RNA-binding proteins. Int J Biol Macromol 40:479–483

Anbarasu A, Prasad VR, Sathpathy S, Sethumadhavan R (2009) Influence of cation–π interactions to the structural stability of prokaryotic and eukaryotic translation elongation factors. Protoplasma 238:11–20

Anitha P, Sivasakthi V, Lavanya P, Bag S, Kumar KM, Anbarasu A, Ramaiah S (2012) Arginine and lysine interactions with π residues in metalloproteins. Bioinformation 8:820–826

Boeckmann B, Bairoch A, Apweiler R, Blatter MC, Estreicher A, Gasteiger E, Martin MJ, Michoud K, O'Donovan C, Phan I, Pilbout S, Schneider M (2003) The SWISS-PROT protein knowledgebase and its supplement TrEMBL in 2003. Nucleic Acids Res 31:365–370

Bogan AA, Thorn KS (1998) Anatomy of hot spots in protein interfaces. J Mol Biol 280:1–9

Borozan SZ, Dimitrijević BP, Stojanović SĐ (2013) Cation–π interactions in high resolution protein–RNA complex crystal structures. Comput Biol Chem 47:105–112

Brocchieri L, Karlin S (1994) Geometry of interplanar residue contacts in protein structures. Proc Natl Acad Sci U S A 91:9297–9301

Chakkaravarthi S, Babu MM, Gromiha MM, Jayaraman G, Sethumadhavan R (2006) Exploring the environmental preference of weak interactions in $(\alpha/\beta)_8$ barrel proteins. Proteins 65:75–86

Chaturvedi UC, Shrivastava R (2005) Interaction of viral proteins with metal ions: role in maintaining the structure and functions of viruses. FEMS Immunol Med Microbiol 43:105–114

Craik DJ, Daly NL, Waine C (2001) The cystine knot motif in toxins and implications for drug design. Toxicon 39:43–60

Crowley PB, Golovin A (2005) Cation–π interactions in protein-protein interfaces. Proteins 59:231–239

DeLano WL (2002) Unraveling hot spots in binding interfaces: progress and challenges. Curr Opin Struct Biol 12:14–20

Dimitrijević BP, Borozan SZ, Stojanović SĐ (2012) π–π and cation–π interactions in protein-porphyrin complex crystal structures. RSC Adv 2:12963–12972

Dosztanyi Z, Fiser A, Simon I (1997) Stabilization centers in proteins: identification, characterization and predictions. J Mol Biol 272:597–612

Dosztanyi Z, Magyar C, Tusnady G, Simon I (2003) SCide: identification of stabilization centers in proteins. Bioinformatics 19:899–900

Elumalai P, Rajasekaran M, Liu HL, Chen C (2010) Investigation of cation–π interactions in sugar-binding proteins. Protoplasma 247:13–24

Fischer S, Benz J, Spath B, Maier LK, Straub J, Granzow M, Raabe M, Urlaub H, Hoffmann J, Brutschy B, Allers T, Soppa J, Marchfelder

A (2010) The archaeal Lsm protein binds to small RNAs. J Biol Chem 285:34429–34438
Gallivan JP, Dougherty DA (1999) Cation–π interactions in structural biology. Proc Natl Acad Sci U S A 96:9459–9464
Gasymov OK, Abduragimov AR, Glasgow BJ (2012) Cation–π interactions in lipocalins: structural and functional implications. Biochemistry 51:2991–3002
Gromiha MM (2003) Influence of cation–π interactions in different folding types of membrane proteins. Biophys Chem 103: 251–258
Gromiha MM, Santhosh C, Suwa M (2004) Influence of cation–π interactions in protein–DNA complexes. Polymer 45:633–639
Guharoy M, Chakrabarti P (2009) Empirical estimation of the energetic contribution of individual interface residues in structures of protein-protein complexes. J Comput Aided Mol Des 23:645–654
Guharoy M, Pal A, Dasgupta M, Chakrabarti P (2011) PRICE (protein interface conservation and energetics): a server for the analysis of protein-protein interfaces. J Struct Funct Genom 12:33–41
Hallowita (2011) Structural and thermochemical studies of cation−π interactions: elucidation of the fundamental interactions that influence their strength and specificity. Dissertation, Wayne State University
Hermann H, Fabrizio P, Raker VA, Foulaki K, Hornig H, Brahms H, Luhrmann R (1995) snRNP Sm proteins share two evolutionarily conserved sequence motifs which are involved in Sm protein-protein interactions. EMBO J 14:2076–2088
Huang H, Rodgers MT (2002) Sigma versus pi interactions in alkali metal ion binding to azoles: threshold collision-induced dissociation and ab initio theory studies. J Phys Chem A 106:4277–8942
Jorgensen WL, Maxwell DS, Tirado Rives J (1996) Development and testing of the OPLS all-atom force field on conformational energetics and properties of organic liquids. J Am Chem Soc 118:11225–11236
Kabsch W, Sander C (1983) Dictionary of protein secondary structure: pattern recognition of hydrogen-bonded and geometrical features. Biopolymers 22:2577–2637
Khusial P, Plaag R, Zieve GW (2005) LSm proteins form heptameric rings that bind to RNA via repeating motifs. Trends Biochem Sci 30: 522–528
Kumpf RA, Dougherty DA (1993) A mechanism for ion selectivity in potassium channels: computational studies of cation–π interactions. Science 261:1708–1710
Lavanya P, Ramaiah S, Anbarasu A (2013) Cation–π interactions in β-lactamases: the role in structural stability. Cell Biochem Biophys 66: 147–155
Li ZH, Liu J, Qiao M, Fan K-N (2009) A theoretical study on the metal cation–π complexes of Zn^{2+} and Cd^{2+} with benzene and cyclohexene. Mol Phys 107:1271–1282
Liao SM, Du QS, Meng JZ, Pang ZW, Huang RB (2013) The multiple roles of histidine in protein interactions. Chem Cent J 7:44
Ma JC, Dougherty DA (1997) The cation–π interaction. Chem Rev 97: 1303–1324
Magyar C, Gromiha MM, Pujadas G, Tusnady GE, Simon I (2005) SRide: a server for identifying stabilizing residues in proteins. Nucleic Acids Res 33:W303–W305
Mahadevi AS, Sastry GN (2013) Cation–π interaction: its role and relevance in chemistry, biology, and material science. Chem Rev 113:2100–2138
Malkov SN, Zivković MV, Beljanski MV, Hall MB, Zarić SD (2008) A reexamination of the propensities of amino acids towards a particular secondary structure: classification of amino acids based on their chemical structure. J Mol Model 14:769–775
Mattaj IW, De Robertis EM (1985) Nuclear segregation of U2 snRNA requires binding of specific snRNP proteins. Cell 40:111–118
McDonald IK, Thornton JM (1994) Satisfying hydrogen bonding potential in proteins. J Mol Biol 238:777–793
Measey TJ, Smith KB, Decatur SM, Zhao L, Yang G, Schweitzer-Stenner R (2009) Self-aggregation of a polyalanine octamer promoted by its C-terminal tyrosine and probed by a strongly enhanced vibrational circular dichroism signal. J Am Chem Soc 131: 18218–18219
Meyer EA, Castellano RK, Diederich F (2003) Interactions with aromatic rings in chemical and biological recognition. Angew Chem Int Ed Engl 42:1210–1250
Mitchell JB, Nandi CL, McDonald IK, Thornton JM, Price SL (1994) Amino/aromatic interactions in proteins: is the evidence stacked against hydrogen bonding? J Mol Biol 239:315–331
Moradi M, Peyghan AA, Bagheri Z, Kamfiroozi M (2012) Cation–π interaction of alkali metal ions with C24 fullerene: a DFT study. J Mol Model 18:3535–3540
Moreira IS, Fernandes PA, Ramos MJ (2007) Hot spots—a review of the protein-protein interface determinant amino-acid residues. Proteins 68:803–812
Mura C, Cascio D, Sawaya MR, Eisenberg DS (2001) The crystal structure of a heptameric archaeal Sm protein: implications for the eukaryotic snRNP core. Proc Natl Acad Sci U S A 98:5532–5537
Murzin AG, Brenner SE, Hubbard T, Chothia C (1995) SCOP: a structural classification of proteins database for the investigation of sequences and structures. J Mol Biol 247:536–540
Peter B, Polyansky AA, Fanucchi S, Dirr HW (2014) A Lys–Trp cation–π interaction mediates the dimerization and function of the chloride intracellular channel protein 1 transmembrane domain. Biochemistry 53:57–67
Phillips JC, Braun R, Wang W, Gumbart J, Tajkhorshid E, Villa E, Chipot C, Skeel RD, Kale L, Schulten K (2005) Scalable molecular dynamics with NAMD. J Comput Chem 26:1781–1802
Priyakumar UD, Punnagai M, Krishna Mohan GP, Sastry GN (2004) A computational study of cation–π interactions in polycyclic systems: exploring the dependence on the curvature and electronic factors. Tetrahedron 60:3037–3043
Ramanathan K, Shanthi V, Sethumadhavan R (2011) A compact review on the comparison of conventional and non-conventional interactions on the structural stability of therapeutic proteins. Interdiscip Sci Rev 3:144–160
Reddy AS, Sastry GM, Sastry GN (2007) Cation-aromatic database. Proteins 67:1179–1184
Reddy AS, Amarnath HS, Bapi RS, Sastry GM, Sastry GN (2008) Protein ligand interaction database (PLID). Comput Biol Chem 32:387–390
Rose PW, Beran B, Bi C, Bluhm WF, Dimitropoulos D, Goodsell DS, Prlic A, Quesada M, Quinn GB, Westbrook JD, Young J, Yukich B, Zardecki C, Berman HM, Bourne PE (2011) The RCSB protein data bank: redesigned web site and web services. Nucleic Acids Res 39: D392–D401
Salgado EN, Faraone-Mennella J, Tezcan FA (2007) Controlling protein-protein interactions through metal coordination: assembly of a 16-helix bundle protein. J Am Chem Soc 129:13374–13375
Salonen LM, Ellermann M, Diederich F (2011) Aromatic rings in chemical and biological recognition: energetics and structures. Angew Chem Int Ed Engl 50:4808–4842
Seraphin B (1995) Sm and Sm-like proteins belong to a large family: identification of proteins of the U6 as well as the U1, U2, U4 and U5 snRNPs. EMBO J 14:2089–2098
Shanthi V, Ramanathan K, Sethumadhavan R (2009) Role of the cation-π interaction in therapeutic proteins: a comparative study with conventional stabilizing forces. J Comput Sci Syst Biol 2:051–068
Singh NJ, Min SK, Kim DY, Kim KS (2009) Comprehensive energy analysis for various types of π-interaction. J Chem Theory Comput 5:515–529
Sophiya K, Anbarasu A (2011) Structural stability studies in adhesion molecules—role of cation–π interactions. Protoplasma 248:673–682

Stewart M, Dunlap T, Dourlain E, Grant B, McFail-Isom L (2013) Cations form sequence selective motifs within DNA grooves via a combination of cation–π and ion-dipole/hydrogen bond interactions. PLoS One 8:e71420

Stojanović SĐ, Zarić BL, Zarić SD (2010) Protein subunit interfaces: a statistical analysis of hot spots in Sm proteins. J Mol Model 16: 1743–1751

Stojanović SĐ, Isenović ER, Zarić BL (2011) Contribution of non-canonical interactions to the stability of Sm/LSm oligomeric assemblies. Mol Inf 30:430–442

Stojanović SĐ, Isenović ER, Zarić BL (2012) Non-canonical interactions of porphyrins in porphyrin-containing proteins. Amino Acids 43: 1535–1546

Tayubi IA, Sethumadhavan R (2010) Nature of cation–π interactions and their role in structural stability of immunoglobulin proteins. Biochemistry (Mosc) 75:912–918

Valentin-Hansen P, Eriksen M, Udesen C (2004) The bacterial Sm-like protein Hfq: a key player in RNA transactions. Mol Microbiol 51: 1525–1533

Vijay D, Sastry GN (2008) Exploring the size dependence of cyclic and acyclic π-systems on cation–π binding. Phys Chem Chem Phys 10: 582–590

Vijay D, Zipse H, Sastry GN (2008) On the cooperativity of cation–π and hydrogen bonding interactions. J Phys Chem B 112:8863–8867

Wang G, Dunbrack RL Jr (2003) PISCES: a protein sequence culling server. Bioinformatics 19:1589–1591

Waters ML (2004) Aromatic interactions in peptides: impact on structure and function. Biopolymers 76:435–445

Zaric B, Chami M, Remigy H, Engel A, Ballmer-Hofer K, Winkler FK, Kambach C (2005) Reconstitution of two recombinant LSm protein complexes reveals aspects of their architecture, assembly, and function. J Biol Chem 280:16066–16075

Zarić BL, Jovanović VB, Stojanović SĐ (2011) Non-covalent interactions across subunit interfaces in Sm proteins. J Theor Biol 271: 18–26

Zhang B, Guan CC, Chen WT, Zhang P, Yan M, Shi JH, Qin CL, Yang Q (2007) A20 inhibits human salivary adenoid cystic carcinoma cells invasion via blocking nuclear factor–κB activation. Chin Med J (Engl) 120:1830–1835

Zhu D, Herbert BE, Schlautman MA, Carraway ER (2004) Characterization of cation–π interactions in aqueous solution using deuterium nuclear magnetic resonance spectroscopy. J Environ Qual 33:276–284